



Piston Slippers for Robust Water Hydraulic Pumps

Florian Schoemacker*, Hubertus Murrenhoff*

RWTH Aachen University, Institute for Fluid Power Drives and Systems (IFAS), Campus Boulevard 30,
D-52074 Aachen, Germany*
E-Mail: Florian.Schoemacker@ifas.rwth-aachen.de

Water hydraulics are used for applications which require an environmental safety standard for the fluid. In comparison to oil, lubrication with water is a challenging aspect because of the fluid's lower viscosity. Wear and leakage in water lubricated contacts require lower pressure loads. In order to estimate the possible load carrying capacity in water hydraulics, the tribological contact between the piston slipper and swash plate in axial piston machine and respectively eccentric shaft in radial piston machines is investigated. For this purpose simulations based on the Reynolds-Equation are carried out and analysed.

Keywords: Water Hydraulics, radial piston pump, piston slipper, hydrostatic compensation, hydrodynamic load carrying capacity

Target audience: Water Hydraulics

1 Introduction

Being mostly replaced by oil-hydraulics, water hydraulics are nowadays still used, e.g., for press and mining applications and in food and pharmaceutic industries. These applications rely on the main advantages of using water as a pressure medium which are that water is not flammable and tap water as a source is non-toxic /2/. In comparison to oil, water also has several disadvantages as being a poor lubricant. Regarding cavitation in hydraulic systems, water has a much higher vapor pressure. Therefore, cavitation more likely occurs, if for example the static pressure locally drops due to high velocities /1/.

A current research project at IFAS focuses on raising the pressure level and therefore the power density of compact piston pumps for water hydraulics using tap water. State of the art water-lubricated axial pistons pumps are only available on the market for a pressure level of maximum 16 MPa. Compared to a 35 MPa pressure level of oil hydraulic pumps, the remaining potential is relatively high (Figure 1). The present limitation is given due to wear and leakage in tribological contacts. In order to raise the pressure level, lubrication with water has to be investigated thoroughly. For the geometry of an axial piston machine a variety of research has already been done.

Manring et al. /3/ investigated the effect of linear deformations using an analytical solution of a hydrostatic slipper bearing. Calculations were done for concave and convex deformations. A convex deformation means that the gap height at the outer radius of the slipper collar is greater than at the inner radius. The deformation of a concave slipper is vice versa. A concave deformation leads to a higher, a convex deformation to a lower load carrying capacity. The leakage is increased in both cases. Within another research project Manring et al. /4/ measured the pressure profile of a hydrostatic slipper bearing. The test bench was equipped with pressure sensors on different radii of the slipper bearing. From the measurements Manring was able to calculate the load carrying capacity. The investigation focused on different ball socket geometries within the piston slipper.

Kazama /5/ developed a simulation model for the slipper/swash plate contact for mixed lubrication. He used the Average Flow Model of Patir and Cheng and the asperity-contacting model of Greenwood and Williamson in his simulation. Therefore this simulation model contains several side-effects that occur during mixed lubrication.

Kazama investigated the effect of an eccentric position of the piston pressure force which leads to greater inclination angles of the slipper and also higher contact pressure.

Liu et al. /6/ developed a test bench for experiments in search for materials for water hydraulic axial piston pumps. The test bench consisted of a turning swash plate (wobble plate) which actuated a piston and its slipper. Therefore the slipper/swash plate contact as well as the piston/cylinder contact could be tested. Liu et al. experimented with slippers made up of PEEK running against metal and ceramic coating. The wear value of the slipper is reduced to 38 % for the ceramic coating (stainless steel 32 μm , ZrO_2 11.9 μm).

Rokala /7/ investigated the contact between slipper and swash plate for axial piston machines in order to verify the function of the tribological contact in a variable displacement water pump. For this purpose he developed a test bench containing a swash plate with a variable angle and a piston/slipper assembly. Rokala measured the gap height of the slipper during operation to be about 7 to 10 μm . Furthermore a simulation of the deformation of the slipper was carried out and the resulting pressure profile was calculated. Rokala concludes that the development of a variable displacement water pump is possible.

The presented literature dealt with axial piston water hydraulic machines (APM). The research at IFAS focuses also on the principle of a radial piston machine (RPM). Radial piston pumps are typically used for high pressure applications, for example in common rail diesel pumps. For this research paper, piston machines with a displacement ranging from 23 cm^3 to 46 cm^3 are considered. The nominal speed is 1500 rpm and the maximum pressure is 21 MPa. The investigation and design of the tribological contact of the piston slipper, i.e., the simulation of the load carrying capacity, is discussed. The aim is to develop a sustainable tribological contact with a reasonable compromise between load carrying capacity and water leakage. The calculations base upon the viscosity of water and respectively HFA fluid. The use of tap water requires a more detailed focus on hydrodynamics because of the lower lubrication condition compared to HFA fluid.

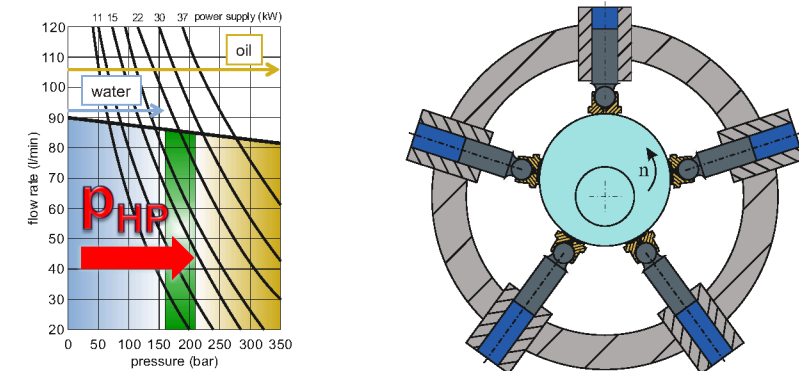


Figure 1: Pressure level for oil and water (left), principle of a radial piston machine (right)

2 Lubrication with Water

Regarding lubrication with water, basically the same conditions as for oil lubrication are given. For the Reynolds-Equation used to describe a sliding wedge contact, the only condition referring to the fluid is that it needs to be Newtonian. Water is a Newtonian fluid. Therefore the same hydrodynamic theory as for oil lubrication can be applied. Due to the lower viscosity compared to oil, the gap height of the fluid film will be reduced in the case of water lubrication. In order to estimate the gap height, a sliding wedge geometry as shown in **Figure 2** is used. Two different methods are compared, demonstrating the gap height's change if the same hydrodynamic pressure built-up is assumed as for using a HLP 32 oil.

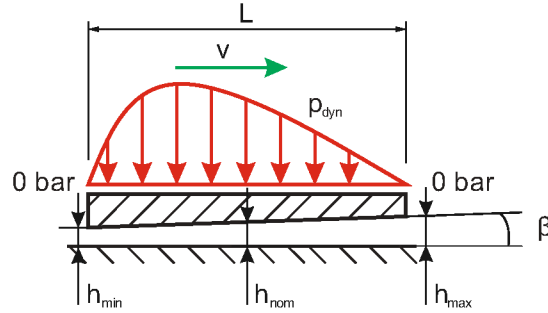


Figure 2: Sliding wedge geometry

Backé /1/ assumes that the change in height of the wedge ($h_{\max} - h_{\min}$) has the same value as the minimum fluid film thickness h_{\min} . Therefore the gap height and also the inclination angle are changed for comparing water to oil lubrication. This assumption leads to the quotient in **Eq. 1**.

$$\frac{h_{\text{Water}}}{h_{\text{Oil}}}\bigg|_{\text{Backé}} = \sqrt{\frac{\mu_{\text{Water}}}{\mu_{\text{Oil}}}} \approx \sqrt{\frac{1}{30}} = 0.18 \quad (1)$$

The fluid film thickness h_{Water} is reduced to 18 % of the film thickness of the HLP 32 oil.

A different method is to assume the same tilting angle for both lubrication models and to change only the gap height. The calculation leads to a quotient in **Eq. 2** for the nominal gap height.

$$\frac{h_{\text{Water}}}{h_{\text{Oil}}}\bigg|_{\text{So}} = \sqrt[3]{\frac{\mu_{\text{Water}}}{\mu_{\text{Oil}}}} \approx \sqrt[3]{\frac{1}{30}} = 0.32 \quad (2)$$

The water fluid film is reduced to 32 % of the oil fluid film. Compared to the first method, the fluid film is 1.78 times as high. Considering that the inclination angle might change as well, the real value of the quotient is assumed to be between these extremes.

Furthermore the reduced fluid film height causes an increased interference with side effects compared to oil-lubricated contacts, e.g., interaction of the surface roughness or elastic deformation due to high loads /1/. Therefore the hydrodynamic load carrying capacity should be considered regarding several aspects. The research focuses on the impact of geometry and gap height on the load carrying capacity.

3 Slipper Geometry and Calculation

The geometry of the two slipper types, axial piston machine (APM) and radial piston machine (RPM), are shown on **Figure 3**.

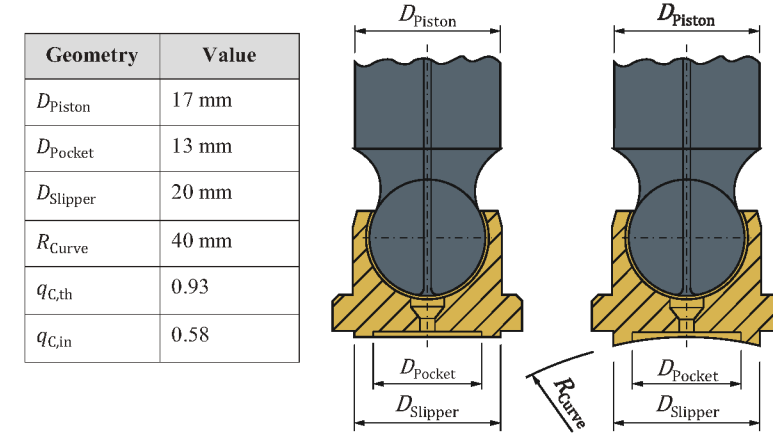


Figure 3: Piston geometry

In the piston slipper contact the load force is usually hydrostatically compensated to a certain degree which reduces the remaining load for the hydrodynamic bearing. The disadvantage of this method is that a hydrostatic compensation causes leakage. In conclusion a compromise has to be found between high load carrying capacity and low leakage. In order to estimate the amount of the hydrostatically compensated load, usually the theoretical compensation is stated as the force ratio $q_{C,\text{th}}$ calculated using **Eq. 3**.

$$q_C = \frac{F_{\text{Fluid}}}{F_{\text{Piston}}} \Rightarrow q_{C,\text{th}} = \frac{p_{\text{HP}} \cdot D_{\text{Pocket}}^2 \cdot \frac{\pi}{4} + \int_{D_{\text{Pocket}}/2}^{D_{\text{Slipper}}/2} \left(p_{\text{HP}} - p_{\text{HP}} \cdot \frac{\ln(2 \cdot r / D_{\text{Pocket}})}{\ln(D_{\text{Slipper}} / D_{\text{Pocket}})} \right) \cdot 2\pi \cdot r \cdot dr}{p_{\text{HP}} \cdot A_{\text{Piston}}} = \quad (3)$$

$$q_{C,\text{th}} = \frac{p_{\text{HP}} \cdot (D_{\text{Slipper}}^2 - D_{\text{Pocket}}^2) \cdot \frac{\pi}{8} / \ln(D_{\text{Slipper}} / D_{\text{Pocket}})}{p_{\text{HP}} \cdot D_{\text{Piston}}^2 \cdot \frac{\pi}{4}} = \frac{D_{\text{Slipper}}^2 - D_{\text{Pocket}}^2}{2 \cdot D_{\text{Piston}}^2 \cdot \ln(D_{\text{Slipper}} / D_{\text{Pocket}})}$$

For this equation the piston slipper has a circular geometry and a logarithmic pressure drop for the sliding surface is assumed. This assumption bases upon a constant gap height, which causes the pressure drop due to leakage, and no sliding motion of the piston. But the remaining, not compensated load would actually close the gap. This means that the theoretical compensation does not apply to real contacts.

Furthermore if the distribution of the gap height is changed (e.g., during motion), the pressure distribution changes as well. Therefore a compensation ratio $q_{C,\text{in}}$ is defined, including only the inner pocket of the slipper pad. This area is independent from any movement and gap height, representing a constant share of the hydrostatic compensation.

$$q_{C,\text{in}} = \frac{F_{\text{Pocket}}}{F_{\text{Piston}}} = \frac{p_{\text{HP}} \cdot D_{\text{Pocket}}^2 \cdot \frac{\pi}{4}}{p_{\text{HP}} \cdot D_{\text{Piston}}^2 \cdot \frac{\pi}{4}} = \left(\frac{D_{\text{Pocket}}}{D_{\text{Piston}}} \right)^2 \quad (4)$$

The comparison between inner ($q_{C,\text{in}} = 0.58$) and total theoretical compensation ($q_{C,\text{th}} = 0.93$) for the chosen geometry indicates that the load carrying capacity depends strongly on the pressure profile over the collar of the slipper. This means that a change occurring during tilting leads to a different load carrying capacity.

Especially for water lubrication the pressure drop over the sliding surface should be calculated using the Reynolds-Equation, Eq. 5.

$$\frac{\partial}{\partial r} \left(r \cdot \frac{h^3}{12 \cdot \mu} \cdot \frac{\partial p}{\partial r} \right) + \frac{\partial}{\partial \varphi} \left(\frac{h^3}{12 \cdot \mu} \cdot \frac{1}{r} \cdot \frac{\partial p}{\partial \varphi} \right) - \frac{u_r}{2} \cdot r \cdot \frac{\partial h}{\partial r} - \frac{u_\varphi}{2} \cdot \frac{\partial h}{\partial \varphi} = \frac{\partial h}{\partial t} \quad (5)$$

For this research the dynamic change of the gap height is neglected ($\frac{\partial h}{\partial t} = 0$). Furthermore ideal smooth surfaces are considered and because no model for solid contact pressure is implemented, only fluid film pressure can be calculated. The Reynolds-Equation is solved based upon a cylindrical coordinate system which fits the geometrical appearance of the fluid film in the slipper contact.

In water hydraulics, plastics are often used as materials. This causes a relatively high deformation compared to metals which could lead to a higher load carrying capacity. In order to allow this increase, the theoretical compensation $q_{C,th}$ is set to a value of about 93 %. The impact of deformation is discussed in detail in section 5.

The described principles of the compensation and load carrying capacity are applied to the slipper contact of a radial piston pump. In this type of machine, the piston slipper is in contact with the eccentric shaft and therefore the surfaces are curved (Figure 4).

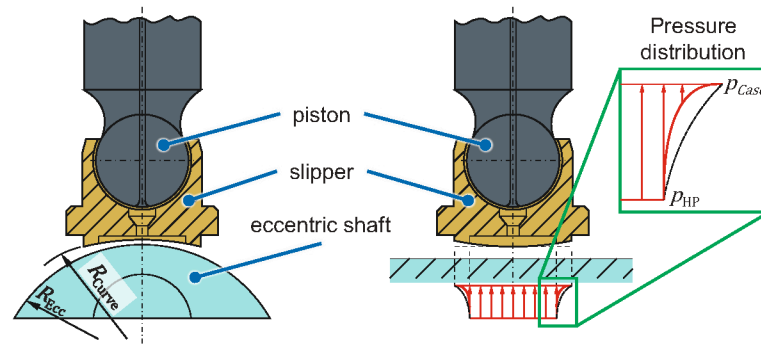


Figure 4: Radial piston slipper (left), unwrapped for calculation (right)

Due to the fact that the concave radius of the slipper R_{Curve} is slightly larger than the convex radius of the shaft R_{Ecc} , the gap height already differs geometrically. This effect is taken into account by calculating the difference of the gap height and using it for an unwrapped simulation. As shown in Figure 4, the assumed logarithmic pressure drop is increased (solid line vs. dashed line). The radial piston machine is investigated with three radius differences ($\Delta R_{RPM} = R_{Curve} - R_{Ecc} = 10, 20$ and $40 \mu m$). If the radius difference is set to zero, the results would be equal to the axial piston slipper.

For all types of slippers the same hydrostatic compensation as shown in Figure 3 is used in order to give a comparison of the load carrying capacity which is given as the effective force ratio $q_{C,eff}$.

$$q_{C,eff} = \frac{F_{Fluid}}{F_{Piston}} = \frac{\int p(r,\varphi) \cdot dA}{p_{HP} \cdot D_{Piston}^2 \cdot \frac{\pi}{4}} \quad (6)$$

4 Results of static Reynolds-Equation

4.1 Parallel Gap

As a reference, a static simulation without an inclination or motion of the slipper is carried out. In this case the results equal the analytical solution which is used for the expression of the theoretical hydrostatic compensation $q_{C,th}$ shown before. The pressure profile depicts a logarithmic pressure drop along the slipper collar, Figure 5. For the simulation a nominal gap height of $0.5 \mu m$ is assumed.

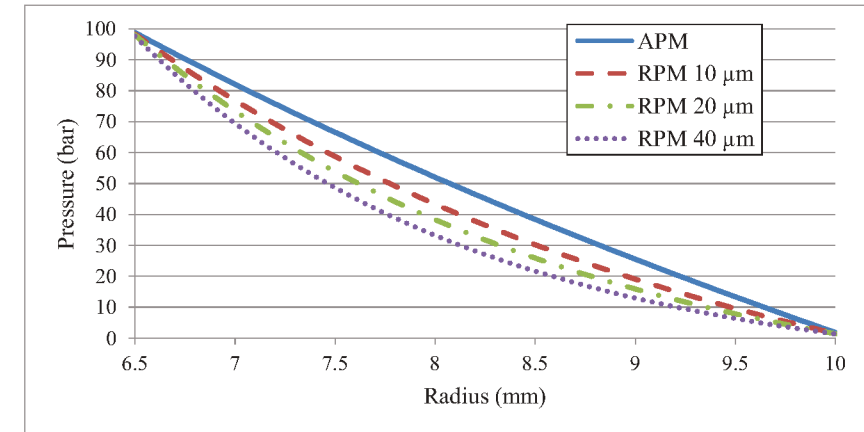


Figure 5: Pressure distribution along the slipper collar ($0.5 \mu m$ gap)

	APM	RPM $10 \mu m$	RPM $20 \mu m$	RPM $40 \mu m$
$q_{C,eff} (-)$	0.932	0.916	0.898	0.876
$Q_{Leak} (ml/min)$	0.088	0.155	0.264	0.632

Table 1: Effective compensation and leakage

The results show that the load carrying capacity given as the value of $q_{C,eff}$ (shown in Table 1) of the radial piston slipper is lower than of the axial piston slipper. Furthermore an increased radius difference ΔR_{RPM} leads to a reduction of the load carrying capacity and an increased leakage. As said before, the results compared to the analytical solution will differ, if the slipper is simulated with an inclination angle and constant motion. This is presented in the following sections.

4.2 Inclination Angle

Once the slipper is tilted against the normal vector of the corresponding surface, the pressure distribution is varied, Figure 6. On one side of the slipper collar the gap height is closing for the leakage flow and on the other side it is opening. Therefore the pressure distribution is unbalanced and able to produce a tilting torque trying to balance the tilting position of the slipper. This means the fluid film bears a normal force as well as a tilting torque.

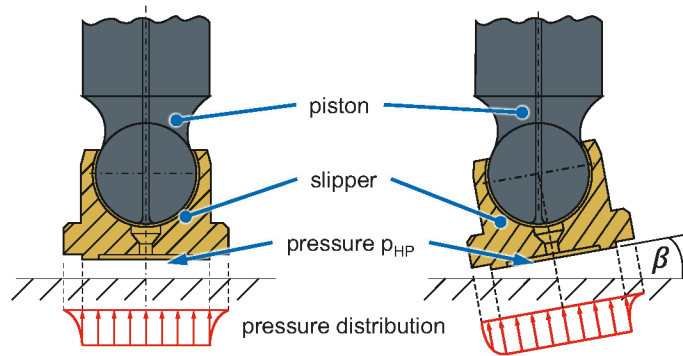


Figure 6: Piston slipper with hydrostatic compensation

To investigate this effect, a simulation with an inclination angle β of 0.001° and a nominal fluid film thickness of $0.5 \mu\text{m}$ is carried out. For the axial piston slipper, gap height and pressure distribution as a result of the simulation can be seen in **Figure 7**. The entire results are shown in **Table 2** on the left. The calculated tilting torque T_{Fluid} is quite low. Because the fluid film is still calculated with no motion, only pressure flow occurs in the Reynolds-Equation. Therefore the resulting pressure distribution is independent of the fluid's viscosity and the results would also apply for oil as a lubrication fluid. However the leakage depends on the viscosity. Due to the difference of the resulting torques and in order to achieve a fair comparison, a simulation with a fixed tilting torque of $T_{\text{Fluid}} = 0.25 \text{ Nm}$ is done and shown on the right-hand side in **Table 2**.

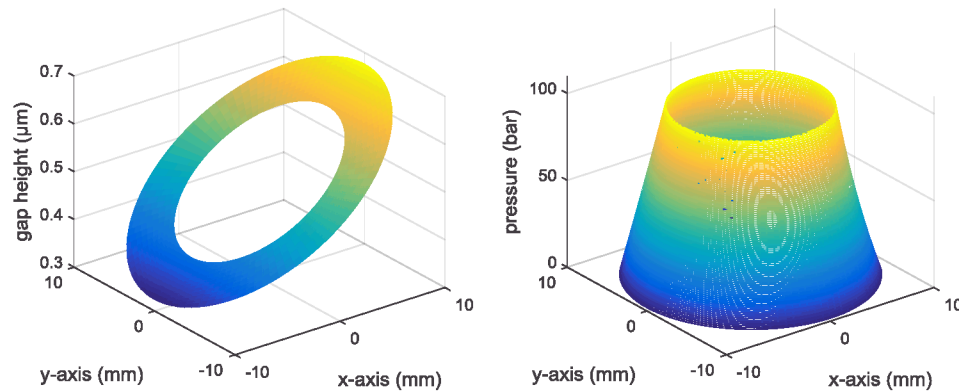


Figure 7: Axial piston slipper: gap height (left) and pressure distribution (right)

	Fixed Inclination Angle ($\beta = 0.001^\circ$)			Fixed Tilting Torque ($T_{\text{Fluid}} = 0.25 \text{ Nm}$)		
	$q_{C,\text{eff}}$ (-)	T_{Fluid} (Nm)	Q_{Leak} (ml/min)	$q_{C,\text{eff}}$ (-)	β ($^\circ$)	Q_{Leak} (ml/min)
APM	0.936	0.246	0.099	0.936	0.00102	0.099
RPM 10 μm	0.917	0.127	0.168	0.920	0.00182	0.198
RPM 20 μm	0.898	0.053	0.280	0.905	0.00362	0.471
RPM 40 μm	0.876	0.002	0.653	0.925	0.00905	2.397

Table 2: Tilting torque ($0.5 \mu\text{m}$ nominal gap height)

The results show that the slippers of the radial piston machine require a greater inclination angle in order to bear the same torque as the axial piston machine's slippers. This means that the ability for bearing tilting torques is higher for axial piston slippers. Eventually the radial piston slipper with a radial difference of $\Delta R_{\text{RPM}} = R_{\text{Curve}} - R_{\text{Ecc}} = 40 \mu\text{m}$ is not able to bear a torque load of 0.25 Nm because due to the large inclination angle the gap height is set to zero at its minimal value (grey shaded cells in **Table 2**). Therefore the fluid film cannot bear the load itself and part of the load is carried by solid metal contact.

4.3 Constant Motion

For the hydrodynamic simulation of the slipper, a constant linear velocity v_{rel} of 1 m/s in direction of the x-axis is assumed. In case of the radial piston machine this value represents a rotational speed of about 500 rpm . At first the same inclination angle of 0.001° as before and a nominal gap height of $0.5 \mu\text{m}$ are used. The plots of this simulation are shown in **Figure 8**. Compared to **Figure 7** the additional pressure built up due to shear flow can be seen.

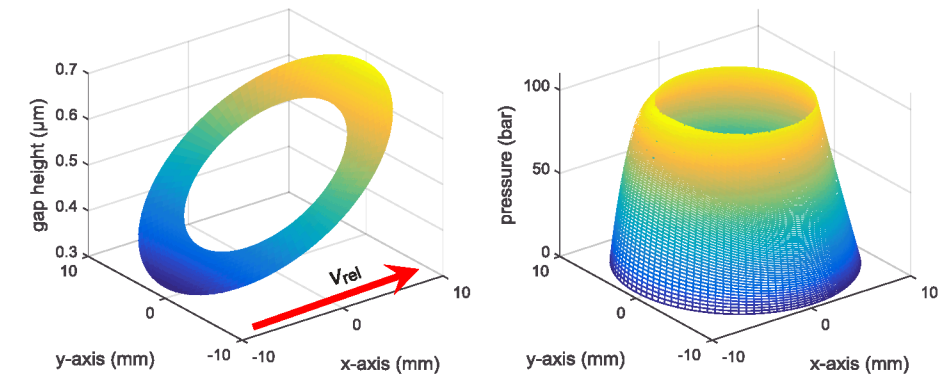


Figure 8: Axial piston slipper: gap height (left) and pressure distribution (right)

For the axial piston machine the simulation results state an already overcompensated force ratio ($q_{C,\text{eff}} = 1.03$). Because of the overcompensation, the nominal gap height is changed to $1 \mu\text{m}$, giving the results shown in **Table 3**. The simulations with a fixed inclination angle show a negative torque for the radial piston machines which means that the assumed inclination angle is too small. Therefore the simulation is also carried out with a fixed tilting torque of 0.15 Nm . In conclusion the load carrying capacity due to the pressure built-up, resulting from of

the shear flow, is increased. The radial piston slipper with $\Delta R_{RPM} = 40 \mu\text{m}$ is not able to carry the tilting torque, even during motion.

	Fixed Inclination Angle ($\beta = 0.001^\circ$)			Fixed Tilting Torque ($T_{\text{Fluid}} = 0.15 \text{ Nm}$)		
	$q_{C,\text{eff}} (-)$	$T_{\text{Fluid}} (\text{Nm})$	$Q_{\text{Leak}} (\text{ml/min})$	$q_{C,\text{eff}} (-)$	$\beta (^\circ)$	$Q_{\text{Leak}} (\text{ml/min})$
APM	0.942	0.156	0.617	0.942	0.00098	0.619
RPM 10 μm	0.933	-0.086	0.837	0.944	0.00237	0.795
RPM 20 μm	0.918	-0.220	1.158	0.936	0.00426	1.254
RPM 40 μm	0.898	-0.296	2.038	0.937	0.00917	3.807

Table 3: Tilting torque (1 μm nominal gap height)

5 Effect of Deformation

The use of plastics as material for water hydraulic components leads to greater deformations compared to metal components used in oil hydraulics. Because the deformations are of the same magnitude as the actual gap height, the effect on the load carrying capacity cannot be neglected. For this approach, the hydrostatic pressure distribution for an axial piston machine is calculated using ideal geometries. Then the deformation due to the pressure distribution is calculated using Ansys FEM. Afterwards the result is used as input for the Reynolds-Equation. This is repeated iteratively until the change of the deformation between two iterations is less than 0.01 μm . The slipper consists of two components: a steel body and an implemented sliding disc made of PEEK. The sliding disc contains the geometry of the collar for the pressurised fluid film.

The deformation of the piston slipper is shown in **Figure 9**. The scale of the deformation is exaggerated by a factor of 550.

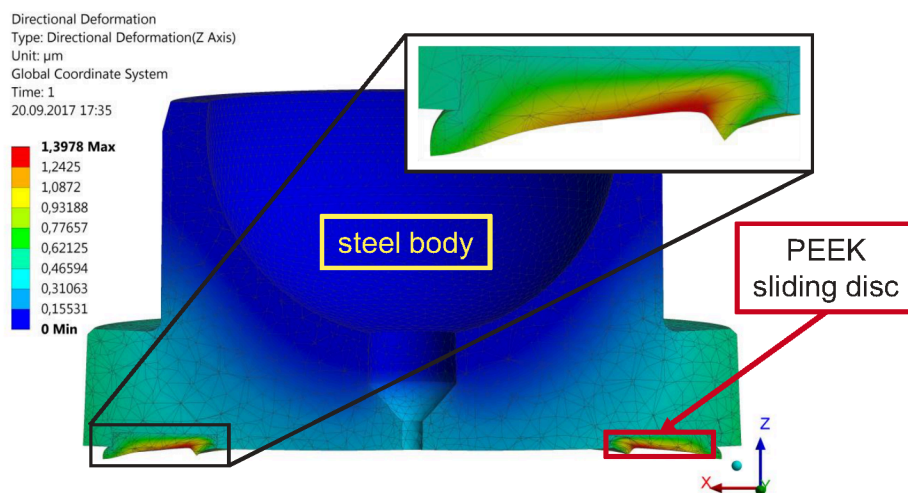


Figure 9: Deformation of the piston slipper (Ansys FEM)

The export of the gap height distribution to the simulation software and the resulting pressure distribution is shown in **Figure 10**.

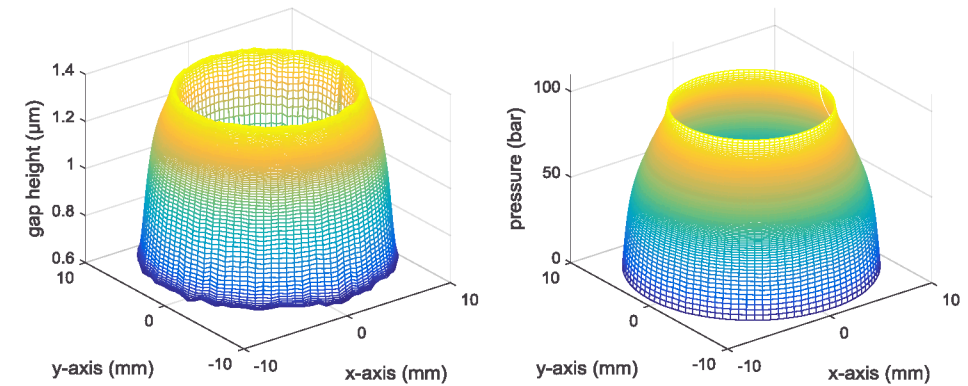


Figure 10: Piston slipper deformation; gap height distribution (left) and pressure distribution (right)

The result of the pressure distribution is comparable to the results of Rokala /7/. The deformation of the slipper results in a load carrying capacity with factor of $q_{C,\text{eff}} = 1.067$, meaning that the slipper is over compensated and therefore will actually open the gap. The leakage value of 0.811 ml/min is increased by factor 5 compared to an undeformed slipper with a gap height of 0.6 μm . The effect of concave deformations which lead to a higher load carrying capacity and also a major increase in leakage fits well to the calculations of Manning /3/.

6 Summary and Conclusion

Due to the relatively low viscosity of tap water, the reduction of the gap height in water-lubricated tribological contacts defines the need for a robust design in water hydraulics. For this purpose the contact between piston slipper and swash plate in axial piston machines and respectively eccentric shaft in radial piston machines has been investigated. The research used a simulation of the hydrodynamic load carrying capacity calculated via the Reynolds-Equation for different operating conditions.

The results indicate that the gap height is in the range of 0.5 μm in order to bear the normal load force and the tilting moment. The axial piston machine's slipper has the greatest overall load carrying capacity. For the radial piston machine the results show that the slippers need to be manufactured with respect to an almost parallel clearance in the lubrication contact. Then the load carrying capacity is of a fair value compared to axial piston machines. The results have not yet been validated via measurements. But compared to oil hydraulics the gap height is reduced due to the lower viscosity of the fluid. The resulting gap height is within the magnitude of the surface roughness which indicates that solid contact and therefore mixed friction will occur in the contact.

Therefore plastic materials are used for water lubricated contacts. The investigation shows that the resulting deformation is of the same magnitude as the gap height itself which affects the fluid film pressure and the load carrying capacity. Due to the use of plastic materials the deformation has already a major impact at relatively low pressures compared to oil hydraulics. In an oil hydraulic piston machine, metal materials can be used for both surfaces and therefore critical deformations occur at much higher pressure levels. But for designing a water lubricated slipper contact, the deformation has to be considered.

Due to the small clearances necessary to ensure a fair load carrying capacity, the micro hydrodynamic effects should be taken into account. This entails an additional pressure built up due to the surface roughness on the one hand and a contact pressure built-up due to solid metal contact on the other. Another option is to use tailored surface textures which lead to a higher hydrodynamic load carrying capacity. Doing so, the already discussed poor lubrication with water needs to be modelled in detail and calculated thoroughly.

7 Acknowledgements

Supported by:



on the basis of a decision
by the German Bundestag

The research work leading to this publication was funded by the German Federal Ministry for Economic Affairs and Energy under the reference ZF4199603KO6 as a cooperation project between Institute of Fluid Power Drives and Systems (IFAS), RWTH Aachen University and Hauhinco Maschinenfabrik GmbH & Co.KG. The responsibility for the content of this paper lies with the authors. The authors are grateful for the funding.

Nomenclature

Variable	Description	Unit
μ_{Water}	Dynamic viscosity of water	(Pa · s)
h_{Water}	Nominal gap height by lubrication with water	(mm)
D_{Piston}	Diameter of piston	(mm)
D_{Pocket}	Diameter of pocket in slipper contact, inner diameter	(mm)
D_{Slipper}	Outer diameter of slipper contact	(mm)
R_{Curve}	Concave radius of the piston slipper	(mm)
R_{Ecc}	Convex radius of the eccentric shaft	(mm)
ΔR_{RPM}	Difference of slipper radius and eccentric shaft radius of an RPM	(μm)
$q_{\text{C,th}}$	Theoretical compensation of normal load force	(-)
$q_{\text{C,in}}$	Compensation ratio of the pocket	(-)
$q_{\text{C,eff}}$	Effective compensation of normal load force	(-)
p_{HP}	Piston displacement chamber pressure	(bar)
$p_{(r,\varphi)}$	Pressure profile in slipper contact	(bar)
A_{eff}	Area in slipper contact for pressure profile	(mm^2)
β	Inclination angle	($^\circ$)
T_{Fluid}	Tilting torque	(Nm)

References

- /1/ Backé, W., *Water- or Oil-Hydraulics in the future*, In: The Sixth Scandinavian International Conference on Fluid Power. Proceedings of the Conference, Tampere, Finland, pp. 51-65, Mai 26-28, 1999.
- /2/ Trostmann, E. et al., *Tap Water as a Hydraulic Pressure Medium*, Marcel Dekker, Inc., New York, 2000.
- /3/ Manring, N.D. et al., *The Impact of Linear Deformations on stationary Hydrostatic Thrust Bearings*, Journal of Tribology, Vol. 124 No. 4, pp. 874-877, 2002.
- /4/ Manring, N.D. et al., *Experimental Studies on the Performance of Slipper Bearings within Axial-Piston Pumps*, In: Journal of Tribology, Vol. 126 No. 3, pp. 511-518, 2004.
- /5/ Kazama, T., *Numerical Simulation of a Slipper Model for Water Hydraulic Pumps/Motors in Mixed Lubrication*, In: Proceedings of the 6th JFPS International Symposium on Fluid Power, Tsukuba, Japan, pp. 509-514, November 7-10, 2005.
- /6/ Liu et al., *Materials screening of matching pairs in a water hydraulic piston pump*, In: Industrial Lubrication and Tribology, Vol. 61 No. 3, pp. 173-178, 2009.
- /7/ Rokala, M., *Analysis of Slipper Structures in Water Hydraulic Axial Piston Pumps*, Dissertation, Tampere University of Technology, Tampere, 2012.